Nanoscale Tectonics: Self-Assembly, Characterization, and Chemistry of a Novel Class of Organoplatinum Square Macrocycles

Joseph Manna, Christopher J. Kuehl, Jeffery A. Whiteford, Peter J. Stang,* David C. Muddiman, Steven A. Hofstadler, and Richard D. Smith

Contribution from the Department of Chemistry, University of Utah, Salt Lake City, Utah 84112, and Molecular Sciences Research Center and Chemical Sciences Department, Pacific Northwest Laboratory, Richland, Washington 99352

Received August 4, 1997[⊗]

Abstract: Six nanoscale molecular squares are reported. They are prepared in essentially quantitative yields via spontaneous self-assembly of preprogrammed 90° angular units with diverse bimetallic linear linkers. Characterization was accomplished with multinuclear NMR and, in two cases, via ESI-FTICR mass spectral data. The size of these novel metallomacrocycles range from 3.6 nm (diagonal) and 2.6 nm (side) for the smallest to 4.7 nm (diagonal) and 3.4 nm (side) for the largest as estimated by extensible systematic force field calculations. The molecular squares incorporating alkynyl units as corners are able to complex four Ag^+ ions via the π-tweezer effect.

Introduction

The use of transition metals in conjunction with multidentate ligands and the concomitant dative bonding as a means to drive and direct the self-assembly of abiotic supramolecular species represents a different and interesting alternative to the biomimetic weak interaction (hydrogen bonding, $\pi-\pi$-stacking, van der Waals interactions, etc.) controlled processes.[1] This methodology has been successfully and reasonably extensively employed in the formation of metal helicates[2] and other two- and three-dimensional metallomacrocycles of diverse shapes and sizes.[3,4] In the last few years we,[5] as well as Fujita and Ogura,[4] have used coordination as the motif for the construction of diverse molecular squares[6] and, most recently, the assembly of molecular hexagons[7] and achiral[8] as well as chiral[9] octahedrons. However, with few exceptions, all of these assemblies are generally smaller than 1 nm in size.

The ultimate goal of much of this research, in common with most of contemporary abiotic supramolecular chemistry, is the design of methodologies and development of technology for the assembly and manufacturing of nanoscale molecular devices and machinery.[10] This of course requires the ability to readily construct nanoscale supramolecular species from simple, easily available precursors. Herein, we report the formation and characterization of nanoscale supramolecular assemblies in the form of nanoscopic, metallocyclic molecular squares using coordination as the motif to drive and direct their preprogrammed self-assembly. We also present electrospray ionization Fourier transform ion cyclotron resonance mass spectrometry (ESI−FTICR) data for the characterization of selected, representative members of these novel nanoscale metallomacrocycles along with their metal complexation with Ag^+.

Results and Discussion

The rational, efficient design of nanoscale molecular squares requires readily available "preprogrammed" building units. Specifically, the assembly of any square requires[11] shape-defining and -directing 90° angular units **A** in combination with

[⊗] Abstract published in *Advance ACS Abstracts,* November 15, 1997.

(1) For key recent reviews, see: (a) *Comprehensive Supramolecular Chemistry*; Lehn, J.-M., Atwood, J. L., Davies, J. E. D., MacNicol, D. D., Vogtle, F. Eds.; Pergamon Press: Oxford, 1996; Vols. 1−11. (b) Lehn, J.-M. *Supramolecular Chemistry: Concepts and Perspectives*; VCH Publishers: Weinheim, 1995. (c) Philip, D.; Stoddart, J. F. *Angew. Chem., Int. Ed. Engl.* **1996**, *35*, 1154−1196. (d) Lawrence, D. S.; Jiang, T.; Levett, M. *Chem. Rev.* **1995**, *95*, 2229−2260.

(2) For reviews, see: (a) Williams, A. *Chem. Eur. J.* **1997**, *3*, 15. (b) Constable, E. C. *Polynuclear Transition Metal Helicates in Comprehensive Supramolecular Chemistry*; Lehn, J.-M., Sauvage, J. P., Hosseini, M. W., Eds.; Pergamon Press: Oxford, 1996; Vol. 9, Chapter 6, p 213. (c) Constable, E. C. *Tetrahedron* **1992**, *48*, 10013−10059.

(3) Baxter, P. N. W. *Metal Ion Directed Assembly of Complex Molecular Architectures and Nanostructures in Comprehensive Supramolecular Chemistry*; Lehn, J. -M., Sauvage, J. P., Hosseini, M. W., Eds.; Pergamon Press: Oxford, 1996; Vol. 9, Chapter 5, p 165.

(4) For reviews, see: (a) Fujita, M. *Coord. Chem. Rev.* **1996**, *148*, 249−264. (b) Fujita, M. *J. Synth. Org. Chem. Jpn.* **1996**, *54*, 953−963.

(5) (a) Stang, P. J.; Fan, J.; Olenyuk, B. *J. Chem. Soc., Chem. Commun.* **1997**, 1453−1454. (b) Stang, P. J.; Cao, D, H.; Chen, K. C.; Gray, G. M.; Muddiman, D. C.; Smith, R. D. *J. Am. Chem. Soc.* **1997**, *119*, 5163−5168. (c) Whiteford, J. A.; Lu, C. V.; Stang, P. J. *J. Am. Chem. Soc.* **1997**, *119*, 2524−2533. (d) Stang, P. J.; Persky, N. E. *J. Chem. Soc., Chem. Commun.* **1997**, 77−78. (e) Manna, J.; Whiteford, J. A.; Stang, P. J. *J. Am. Chem. Soc.* **1996**, *118*, 8731−8732. (f) Whiteford, J. A.; Rachlin, E.; Stang, P. J. *Angew. Chem., Int. Ed. Engl.* **1996**, *35*, 2524−2529. (g) Stang, P. J.; Whiteford, J. A.; Olenyuk, B. *J. Am. Chem. Soc.* **1996**, *118*, 8221−8230. (h) Stang, P. J.; Whiteford, J. A. *Res. Chem. Intermed.* **1996**, *22*, 659−665. (i) Stang, P. J.; Olenyuk, B.; Fan, J.; Arif, A. M. *Organometallics* **1996**, *15*, 904−908. (j) Stang, P. J.; Olenyuk, B. *Angew. Chem., Int. Ed. Engl.* **1996**, *35*, 732−736. (k) Stang, P. J.; Chen, K.; Arif, A. M. *J. Am. Chem. Soc.* **1995**, *117*, 8793−8797. (l) Stang, P. J.; Cao, D. H.; Saito, S.; Arif, A. M. *J. Am. Chem. Soc.* **1995**, *117*, 6273−6283. (m) Stang, P. J.; Chen, K. *J. Am. Chem. Soc.* **1995**, *117*, 1667−1668. (n) Stang, P. J.; Whiteford, J. A. *Organometallics* **1994**, *13*, 3776−3777. (o) Stang, P. J.; Cao, D. H. *J. Am. Chem. Soc.* **1994**, *116*, 4981−4982.

(6) See also: (a) Slone, R. V.; Hupp, J. T.; Stern, C. L.; Albrecht-Schmitt, T. E. *Inorg. Chem.* **1996**, *35*, 4096−4097. (b) Slone, R. V.; Yoon, D. I.; Calhoun, R. M.; Hupp, J. T. *J. Am. Chem. Soc.* **1995**, *117*, 11813−11814. (c) Rauter, H.; Hillgeris, E. C.; Erxleben, A.; Lippert, B. *J. Am. Chem. Soc.* **1994**, *116*, 616−624. (d) Stricklen, P. M.; Volcko, E. J.; Verkade, J. G. *J. Am. Chem. Soc.* **1983**, *105*, 2494−2495. (e) Drain, C. M.; Lehn, J.-M. *J. Chem. Soc., Chem. Commun.* **1994**, 2313−2313.

(7) Stang, P. J.; Persky, N. E.; Manna, J. *J. Am. Chem. Soc.* **1997**, *119*, 4777−4778.

(8) Fujita, M.; Oguro, D.; Miyazawa, M.; Oka, H.; Yamaguchi, K.; Ogura, K. *Nature* **1995**, *378*, 469−471.

(9) Stang, P. J.; Olenyuk, B.; Muddiman, D. C.; Wunschel, D. S.; Smith, R. D. *Organometallics* **1997**, *16*, 3094−3096.

(10) (a) Ball, P. *Designing the Molecular World*; Princeton University Press: Princeton, NJ, 1994. (b) Drexler, K. E. *Nanosystems: Molecular Machinery, Manufacturing, and Computation*; Wiley: New York, 1992.

(11) Stang, P. J.; Olenyuk, B. *Acc. Chem. Res.* **1997**, *30*. In press.

S0002-7863(97)02668-1 CCC: $14.00

Scheme 1

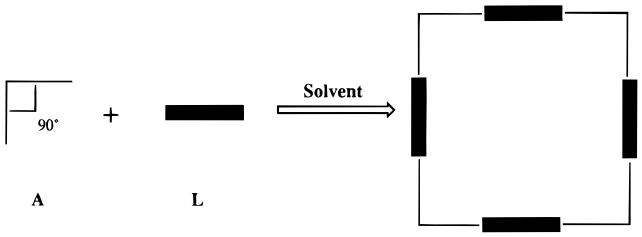

linear linker units **L** as illustrated in Scheme 1. Such a design allows for ready variation of size by (a) different types and sizes of corner units and (b) differing lengths of linker units **L**. The desired linear linkers consist of readily available bimetallic units as described below and summarized in Scheme 2.

Preparation of Bimetallic Linear Linker Units L. Reaction of the previously reported[12] bis(*trans*-Pt$(PR_3)_2$I)aryl complexes **1**−**4** with a slight stoichiometric excess (2.1 equiv) of silver triflate at 0 °C in a methylene chloride solution yielded the *trans* bistriflate complexes **5**−**8** in good yield (Scheme 2), following the workup described in the Experimental Section. The off-white 4,4′-biphenyl- and 4,4″-ter-phenyl-substituted complexes, with PPh_3 ancillary ligands coordinated to platinum, are soluble and partially soluble, respectively, in $CHCl_3$ and CH_2Cl_2. Whereas, the white 1,4-benzene and 4,4′-biphenyl derivatives, with PEt_3 ancillary ligands coordinated to platinum, are soluble in $CHCl_3$ and CH_2Cl_2, insoluble in hexanes, and partially soluble in diethyl ether and acetone. Complexes **5**−**8** were fully characterized by FT-IR spectrometry, NMR spectroscopy (^{1}H, ^{13}C{^{1}H}, ^{19}F{^{1}H}, and ^{31}P{^{1}H}), FAB mass spectrometry, elemental analysis, and physical means. These complexes are oxygen stable for short periods of time; however, they are hygroscopic. The *all-trans* nature of the phosphine ligands at the metal center is unambiguously proven by our observation of a singlet, with concomitant platinum satellites, in the ^{31}P NMR spectra. We do not observe any *trans* to *cis* rearrangement for these complexes, even after prolonged time in solution. A *cis* geometry would be evident by observation of two sets of doublets in the ^{31}P{^{1}H} NMR spectra.

The ^{31}P{^{1}H} NMR chemical shifts for the PEt_3 derivatives **5** and **6** differ significantly from those of the PPh_3 derivatives **7** and **8**. The latter complexes are observed as singlets, coincidentally identical, at 29.3 ppm ($^1J_{PPt}$ = 3219 Hz (**7**), 3198 Hz (**8**)); whereas the PEt_3 complexes are observed at 21.58 (**5**) and 24.97 ppm (**6**) with $^1J_{PPt}$ of 2882 and 2838 Hz, respectively. The ^{31}P{^{1}H} NMR chemical shift and single-bond platinum−phosphorus nuclei spin−spin coupling constant are two of several critical parameters examined for the characterization of the novel, self-assembled architectures to be presented. As was expected, the bistriflate complexes **5**−**8** exhibit singlet signals between −76 and −78 ppm in the ^{19}F{^{1}H} NMR, referenced to external $CFCl_3$.

The proton NMR signals of complexes **5**−**8** are also diagnostic of the *trans*-Pt$(PR_3)_2$-substituted nature of the 1,4-benzene, 4,4′-biphenyl, and 4,4″-ter-phenyl moieties. The aromatic hydrogen of complex **5** dissolved in CD_2Cl_2 is observed as a pseudosinglet at 6.79 ppm in the ^{1}H NMR with coupling to platinum across three bonds. The hydrogens of the biphenyl linkage of complexes **6** and **7** are observed as two sets of doublets in the NMR. The *ortho* and *meta* hydrogens are magnetically coupled to each other over three bonds with a spin−spin coupling constant of 8.2−8.4 Hz. The *ortho* hydrogens signals, 7.29 (**6**) and 6.40 ppm (**7**), are easily distinguished from the *meta* hydrogen signals, 7.18 (**6**) and 5.96 ppm (**7**), by the accompanying platinum satellites ($^3J_{HPt}$) for the former signals of 76 and 60 Hz, respectively. Finally, the hydrogens of the 4,4″-ter-phenyl moiety of **8** are characterized by three unique signals. The interior hydrogen (H_γ) is observed as a singlet at 7.20 ppm in CD_2Cl_2. The *ortho* and *meta* hydrogen signals of **8** mirror those observed for **7**, with chemical shifts of 6.55 and 6.29 ppm, respectively. The chemical shifts of the ancillary PEt_3 and PPh_3 hydrogens are unexceptional and are listed in the Experimental Section.

The corner subunits **9** and **10** (Schemes 3 and 4) have been described previously[5c] and have been utilized in the construction of smaller self-assembled cationic molecular squares.[5c,k]

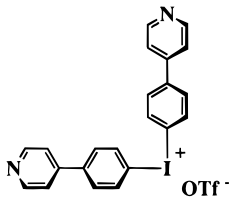

9

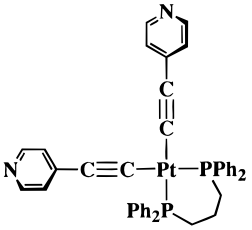

10

Spontaneous Self-Assembly of Nanoscale Molecular Squares. The preparation of several discrete nanoscale platinum macrocyclic complexes can be achieved with surprising simplicity and, when the proper conditions are employed, in essentially quantitative yield in all cases. Due to the highly ionic, charged, nature of the macrocycles studied, all manipulations were undertaken in an inert atmosphere drybox.

Addition of a CD_2Cl_2 solution of the neutral *cis*-Pt(dppp)-$(C{\equiv}CPy)_2$ **10** to the solid bistriflate monomer **5** results in the quantitative formation of the smallest macrocycle of the type described in this paper, structural motif **11**. In a similar manner, addition of a solution of the corner **10** to pure linear monomers **6**, **7**, and **8** yielded the nanoscale macrocycles **12**, **13**, and **14**, respectively, (Scheme 3) of differing topology and dimensions. Interestingly, we found that the self-assembly of macrocycle **13** was concentration dependent. If a 2.0×10^{-2} M CD_2Cl_2 solution of corner **10** was added to a 2.0×10^{-2} M solution of linear linkage **7** in CD_2Cl_2, a mixture of two products form; however, neither product is oligomeric in nature. One of the products is indeed macrocycle **13** (70%); whereas the other product is as yet a structurally unidentifiable macrocycle (30%). If the tectonics is performed by the addition of a concentrated solution of **10** (4.0×10^{-2} M) to solid **7**, then only one product is obtained, macrocycle **13**.

It has been demonstrated that in certain systems the formation of macrocycle versus polymer is, as might be expected, concentration dependent. For example, Hunter and co-workers[13] showed that, at low concentration, monomer is prevalent in solution, while at higher concentration tetramer formation is preferred. At even greater concentration, polymer formation is expected. In contrast, our results for **13** indicate that at higher concentration the simplest macrocycle expected is formed while in a dilute solution the product distribution includes a higher order more complex system. These results indicate that at the present time we lack a correct model that fully describes the self-assembly process for our nanoscale macrocycles.

Addition of a acetone/CH_2Cl_2 solution of iodonium subunit **9** to CH_2Cl_2 solutions of the *trans* bistriflate linkers **5** and **7** results in ready assembly of the macrocycles **15** and **16**,

(12) Manna, J.; Kuehl, C. J.; Whiteford, J. A.; Stang, P. J. *Organometallics* **1997**, *16*, 1897−1905.

(13) Chi, X.; Guerin, A. J.; Haykock, R. A.; Hunter, C. A.; Sarson, L. D. *J. Chem. Soc., Chem. Commun.* **1995**, 2563−2565.

Scheme 2

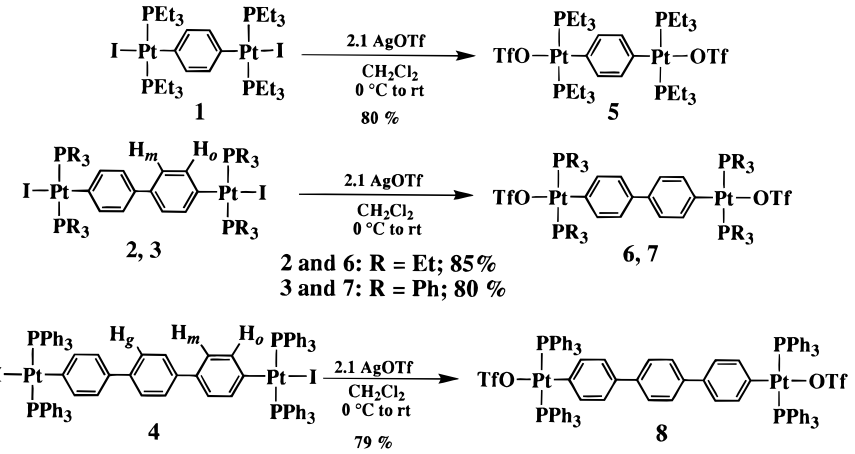

Scheme 3

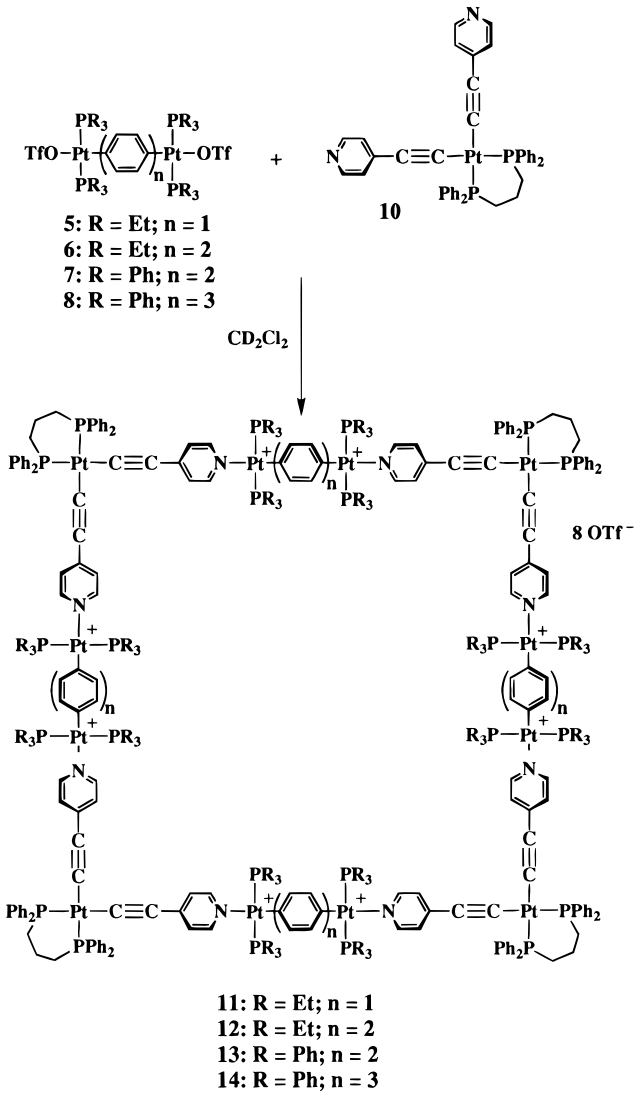

respectively. These self-assemblies proved to be concentration independent, yielding only a single desired product in both cases.

The new macrocycles prepared were characterized by FT-IR spectroscopy, NMR spectroscopy (^{1}H, ^{13}C{^{1}H}, ^{19}F{^{1}H}, and ^{31}P{^{1}H}), elemental analysis, and physical means as described in the Experimental Section. For macrocycles **13** and **16**, these systems were additionally probed by ESI−FTICR mass spectrometry (*vide infra*). The formation of these macrocycles was most easily monitored by examination of the ^{1}H and ^{31}P{^{1}H} NMR spectra. For example, the ^{31}P{^{1}H} NMR of macrocycle **11** exhibits two sharp singlets with a 2:1 intensity ratio at 14.33 ppm ($^1J_{PPt}$ = 2722 Hz) and −5.83 ppm ($^1J_{PPt}$ = 2172 Hz) that are assignable to the *cis*-dppp and *trans*-Pt(PEt_3)$_2$ units, respectively. These values are shifted considerably from those of the pure precursors **5** (21.58 ppm, $^1J_{PPt}$ = 2882 Hz) and **10** (−3.1 ppm, $^1J_{PPt}$ = 2185 Hz). Comparable upfield shifts in the ^{31}P{^{1}H} NMR spectra of the *cis* and *trans* phosphorus signals are observed for **12**−**14**. For the macrocycles incorporating the iodonium modules, as expected, only a singlet is observed due to the *trans* phosphorus ancillary ligands. The ^{31}P{^{1}H} NMR spectrum of molecular squares **15** and **16** display a singlets at 14.2 ppm ($^1J_{PPt}$ = 2720 Hz) and 22.5 ppm ($^1J_{PPt}$ = 3076 Hz). The former values are akin to those for the *trans*-Pt(PEt_3)$_2$ moiety of macrocycle **11**.

Examination of the ^{1}H NMR spectra of these macrocycles reveals significant spectroscopic differences from their pure monomeric subunits. While the chemical shifts of the hydrogens of the ancillary ligands (dppp, PEt_3, and PPh_3) differ only slightly from those of the precursor building blocks, the chemical shifts of the macrocyclic framework 4-(4-bromophenyl)pyridine, 4-alkynylpyridine, 1,4-benzene, 4,4′-biphenyl, and 4,4″-terphenyl) hydrogens are in most cases significantly shifted. For macrocycle **11**, the α and β hydrogens of the pyridyl fragment are observed at 8.20 and 6.87 ppm, respectively, with a $^3J_{HH}$ coupling of 6.0 Hz, in contrast to chemical shifts of 8.20 and 6.62 ppm, respectively, observed for the free corner **10**. The hydrogen of the benzene linker for **11** is observed at 6.96 ppm, shifted downfield by 0.17 ppm from free **5**. Similar chemical shifts for the α and β hydrogens of the orthogonal directing corner are observed for system **12**. Unfortunately, the hydrogens of the biphenyl unit of **12** are partially obscured by the dppp aryl hydrogens. For squares **13** and **14**, the α and β hydrogens of the pyridyl unit are translated 0.67−0.63 and 0.74−0.72 ppm upfield, respectively, from the free ligand **10**. While it might be reasoned that these large shifts are a consequence of the anisotropic ring current of the PPh_3 group versus that of PEt_3, an equally plausible explanation of the greater pyridyl hydrogen shifts might be the increased electrophilicity of monomer **7** and **8** versus that of **5** and **6**, as a consequence of the greater s-donor ability of PEt_3 over PPh_3. The *ortho* and *meta* hydrogens of macrocycles **13** and **14**, are translated down field by 0.27 (**13**) or 0.23 (**14**) and 0.34 (**13**) or 0.28 (**14**) ppm, respectively, relative to the free linear linkers.

The ^{13}C{^{1}H} NMR data for these macrocycles are consistent with our structural formulation. The resonances assigned to iodonium corner **9** and the *cis*-Pt(dppp)(4-C≡CPyr) **10** parallel the values observed for other previously reported[5c,k] molecular

Scheme 4

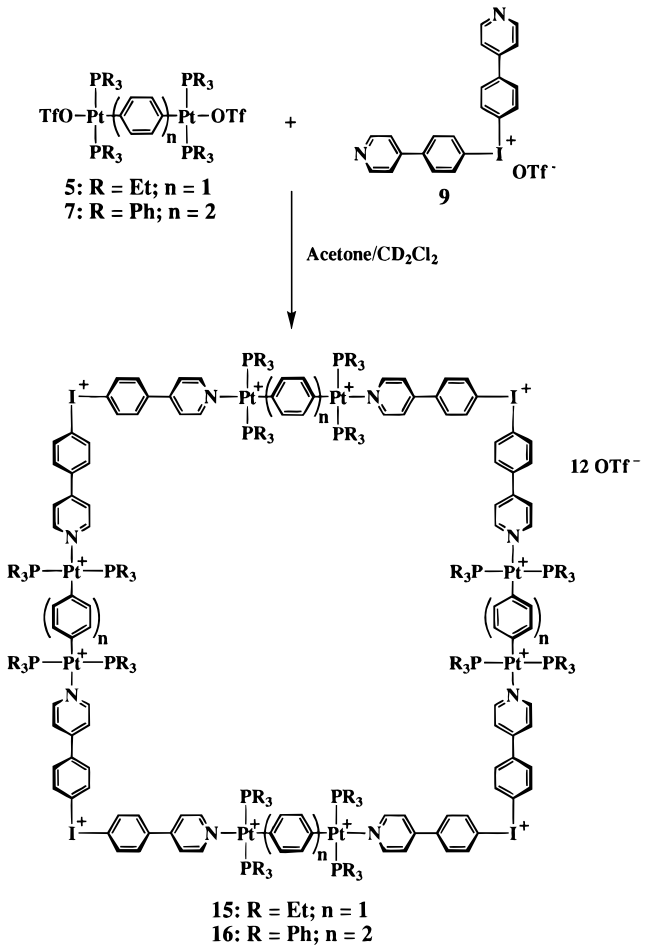

squares incorporating fragments **9** and **10**. Furthermore, the resonances of the linear linkers for these macrocycles are clearly distinct from those of the monomer bistriflate complexes. Moreover, the $^{13}C\{^1H\}$ NMR data of the 4,4′-bis(*trans*-$Pt(PPh_3)_2$)biphenyl subunit of **13** is nearly identical to the data reported for the pyridine adduct 4,4′-bis(*trans*-$Pt(PPh_3)_2$-(pyridine))biphenyl. Finally, the triflate resonance in the $^{19}F\{^1H\}$ NMR is observed as a singlet between −76 and −79 ppm, respectively, referenced to external $CFCl_3$.

These nanoscale macrocycles were found to vary in color from light-yellow for the systems with corner **9** to orange-yellow for the structures incorporating the alkynyl corner **10**. The macrocycles with the iodonium subunits were found to be soluble in acetone and insoluble in ether, methylene chloride, and chloroform. The macrocycles with the alkynyl pyridyl units **10** were found to be soluble in methylene chloride and insoluble in chloroform, hexanes, and diethyl ether.

In order to get a rough idea of the expected dimension of these new macrocycles, the simplest macrocycle prepared, **11**, was structurally minimized by employing the computer modeling program Biosym.[14] Admittedly, the computer model is not as informative as an accurate X-ray crystal structure in regard to the evaluation of subtle electronic and steric effects. However, the model should give reasonably accurate dimensions for the system. Figure 1 displays the minimized van der Waals space-filling model for macrocycle **11**. The calculated dimensions between each diagonal *cis*-Pt center is ∼36 Å, while the distance from *cis*-Pt to *cis*-Pt along the sides of the system is ∼26 Å. As expected, the smallest macrocycle of this class is considerably larger than any of the previously reported systems. Our estimate of the dimensions of **14** are 5 nm diagonally and 3.4 nm along the edge.

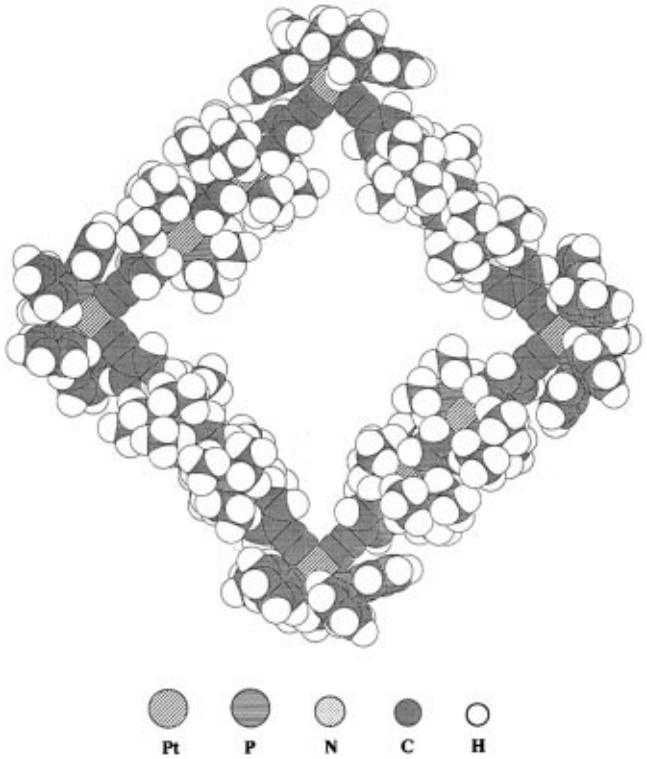

Figure 1. Space-filling model of cationic portion of macrocycle **11**, obtained from ESFF simulations. The view is along the main axis of the molecule.

ESI−FTICR−MS of Selected Nanoscale Systems. Structural elucidation of the macrocyclic architectures presented in this study was firmly achieved by mass spectrometry. Electrospray ionization (ESI), a gentle ionization technique, coupled with Fourier transform ion cyclotron resonance (FTICR) provides charge state and isotopic resolution which allows direct charge state determination.[15]

The upper mass spectrum of Figure 2 shows the isotopically resolved ESI−FTICR mass spectrum obtained from macrocycle **13** using the selected ion accumulation method[16−18] clearly defining the tetrameric nature of the macrocycle. The isotopically resolved signal centered at *m/z* 2012 corresponds to the $[M - 5\ OTf]^{5+}$ charge state species. The charge state was determined by examining the isotopic distribution and the relationship: charge state = 1/(*m*/*z*) spacing. The mass of the 5+ ion was determined to be 10 060.15 Da (i.e., discrete macrocycle and three triflates minus five of the triflate counter anions) which is in good agreement with the theoretical mass of 10 060.03 Da with a mass error of ∼12 ppm.

The lower spectrum of Figure 2 shows the tandem-MS obtained after a sustained off-resonance irradiation (SORI) dissociation event was introduced to fragment the 5+ charge

(14) (a) Dinur, U.; Hagler, A. T. Approaches to Empirical Force Fields. In *Review of Computational Chemistry*; Lipkowitz, K. B., Boyd, D. B., Eds.; VCH: New York, 1991; Vol. 2, Chapter 4. (b) Maple, J. R.; Thacher, T. S.; Dinur, U.; Hagler, A. T. *Chem. Des. Automat. News* **1990**, *5*, 5. (c) Ermer, O. *Struct. Bonding* **1976**, *27*, 161.

(15) Vorm, O.; Roepstorff, P.; Mann, M. *Anal. Chem.* **1994**, *66*, 3281−3287.

(16) Winger, B. E.; Hofstadler, S. A.; Bruce, J. E.; Udseth, H. R.; Smith, R. D. *J. Am. Mass Spectrom.* **1993**, *4*, 566−577.

(17) Gale, D. C.; Smith, R. D. *Rapid Commun. Mass Spectrom.* **1993**, *7*, 1017.

(18) Bruce, J. E.; Vanorden, S. L.; Anderson, G. A.; Hofstadler, S. A.; Sherman, M. G.; Rockwood, A. L.; Smith, R. D. *J. Mass Spectrom.* **1995**, 30, 124−133.

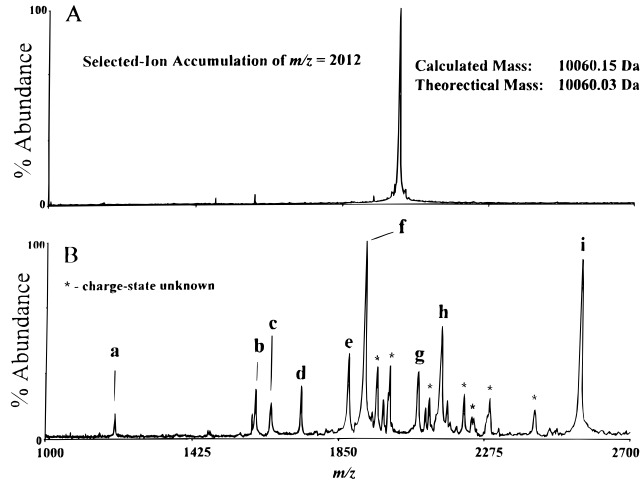

Figure 2. (A) Isotopically resolved ESI−FTICR mass spectrum of macrocycle **13**. (B) Tandem-MS obtained after a sustained off-resonance irradiation (SORI) dissociation event.

Table 1. Structural Assignments from (ESI-FTICR)[2] Mass Spectrum of Macrocycle **13**

peak label	*m/z*	*z*	assignment[a]	mass (obsd)[b]	mass (calcd)[b]	error (ppm)
a	1201.245	2	1C + 1L	2402.49	2402.54	21
b	1607.406	2	2C + 1L	3214.81	3214.74	22
c	1651.684	3	2C + 2L + 1T	4955.05	4955.04	2
d	1720.280	1	1L + 1T	1740.28	1740.31	17
e	1876.788	4	3C + 3L + 2T	7507.15	7507.54	52
f	1922.445	3	3C + 2L + 1T	5767.34	5767.23	19
g	2079.838	4	4C + 3L + 2T	8319.35	8319.73	46
h	2146.355	2	1C + 2L + 2T	4292.71	4292.81	23
i	∼2552[c]	1	1C + 1L + 1T		2551.50	
i	∼2552[c]	2	2C + 2L + 2T		5103.99	

[a] C = corner **10**; L = linker **7**; T = triflate ion. [b] Based on most abundant isotope. [c] Nominal *m/z*; mixture of two (or more) fragment ions.

state of the macrocycle.[17] The structure was elucidated by mass transformation of the ion fragments (i.e., converting *m/z* to the molecular weight domain) utilizing the above relationship and is labeled in the figure. For each ion fragment, charge balance was consistent with the proposed structure. For example, the ion fragment centered around *m/z* 1877 was determined to be a 4+ charge state ion which clearly indicated this fragment contained three corners (**10**), three linkers (**7**−2OTf), and two triflate counteranions. Since each linker contains two *trans* platinum centers, the neutral molecule should have six triflates. However, since this is the 4+ charge state, there should be a mass deficit corresponding to two triflates, which is indeed the case. This confirms the proposed charging mechanism in the electrospray ionization process that the loss of each triflate contributes to a single charge on the molecule. Thus, for each charge observed, there is a loss of 149 Da for the charging mechanism. Table 1 lists the structural assignments, with observed and calculated masses, from the tandem mass spectrum. The fragment ions that were not isotopically resolved were not assigned. Moreover, it is important to note that on the basis of our structure assignment we would not expect to observe any identifiable fragments of the of the type (a) three linkers and one corner or (b) three corners and one linker. One might only expect to see these masses if "aggregation" occurred. Examination of the tandem mass spectrum of **13** revealed no assignable features that could be accountable to such fragments.

Figure 3 displays the ESI-FTICR mass spectrum of **16**. The peak at *m/z* = 1500 is isotopically resolved (*m/z* spacing of 1/6) allowing direct charge state assignment as the 6+ charge

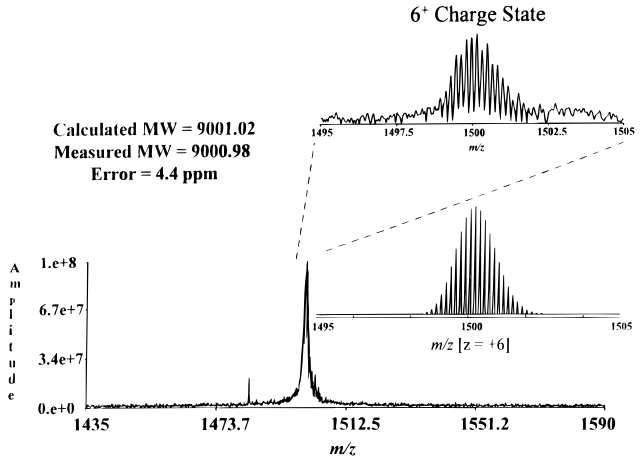

Figure 3. ESI−FTICR mass spectrum of **16**.

state. Since each charge corresponds to the loss of a single triflate ion group, a charge of 6+ is expected to correspond to the intact macrocycle minus six triflates. The expected molecular weight of the intact macrocycle minus the six triflates is 9001.02 (most abundant isotope) and the experimental molecular weight was determined to be 9000.98 (error = 4.4 ppm). As shown in Figure 3, the mass measurement is in excellent agreement with the predicted mass which allows assignment to the product molecule.

Lewis Acid−Base Coordination Chemistry of Nanoscale Macrocycles 11 and 13. It has recently been demonstrated that self-assembled molecular squares employing the bis alkynyl corner **10** are useful Lewis bases for binding electropositive metal guests such as silver triflate (Lewis acid).[5c] For example, it was proven by a full range of spectroscopic methods, as well as mass spectrometry, that a mixed, neutral-charged Pt−Pt or Pt−Pd macrocycles incorporating two corners of type **10** can bind a single Ag cation at each corner by the "π-tweezer effect". This concept has been fully explored by the studies of Lang and co-workers.[19] In a similar manner, we investigated the possibility of observing analogous π-alkynyl silver coordination for macrocycles **11** and **13**.

Addition of slightly more than 4 equiv of silver triflate to the nanoscale systems **11** and **13** resulted in the quantitative formation of silver adducts **17** and **18** (Scheme 5). These complexes were also characterized by spectroscopic, analytical, and physical means. Several spectroscopic parameters undergo considerable modulation due to the coordination of the alkynyl moiety to the silver cation. For example, ν(C≡C) for **17** is observed as a broad singlet at 2086 cm^{-1} in the FT-IR spectrum versus 2119 cm^{-1} observed for macrocycle **13**. Furthermore, significant shifts, relative to **13**, are observed in the ^{31}P{^{1}H} NMR spectrum of **18** for the *cis*-Pt(dppp) resonance. This signal is translated upfield to −9.0 ppm ($^{1}J_{PPt}$ = 2359 Hz), while that of the *trans*-Pt(PPh$_3$)$_2$ signal is nearly unchanged at 20.5 ppm ($^{1}J_{PPt}$ = 3048 Hz). The decrease in ν(C≡C) and large increase in $^{1}J_{PPt}$ (*cis*-Pt(dppp) of **18**, versus that of **13**, is primarily accountable to the decrease in electron density of the alkynyl unit on coordination to silver and, hence, the weakened *trans* influencing ability of C≡CPy on the dppp phosphorus−platinum bond. The ^{13}C{^{1}H} NMR data of the silver-bound corner **10** incorporated into square **18** are akin to the values reported for the mixed, neutral-charged Pt−Pt−Ag macrocycles.[5c]

(19) (a) Janssen, M. D.; Herres, M.; Zsolnai, L.; Spek, A. L.; Grove, D. M.; Lang, H.; van Koten, G. *Inorg. Chem.* **1996**, *35*, 2476−2483. (b) Lang, H.; Weinmann, M. *Synlett* **1996**, 1−10. (c) Janssen, M. D. *Structural Aspects and Reactivity of Self-Assembling Organocopper and Copper Arenethiolate Aggregates*; Thesis Universiteit Utrecht, 1996; p 152. (d) Lang, H.; Blau, S.; Pritzkow, H.; Zsolnai, L. *Organometallics* **1995**, *14*, 1850−1854.

Scheme 5

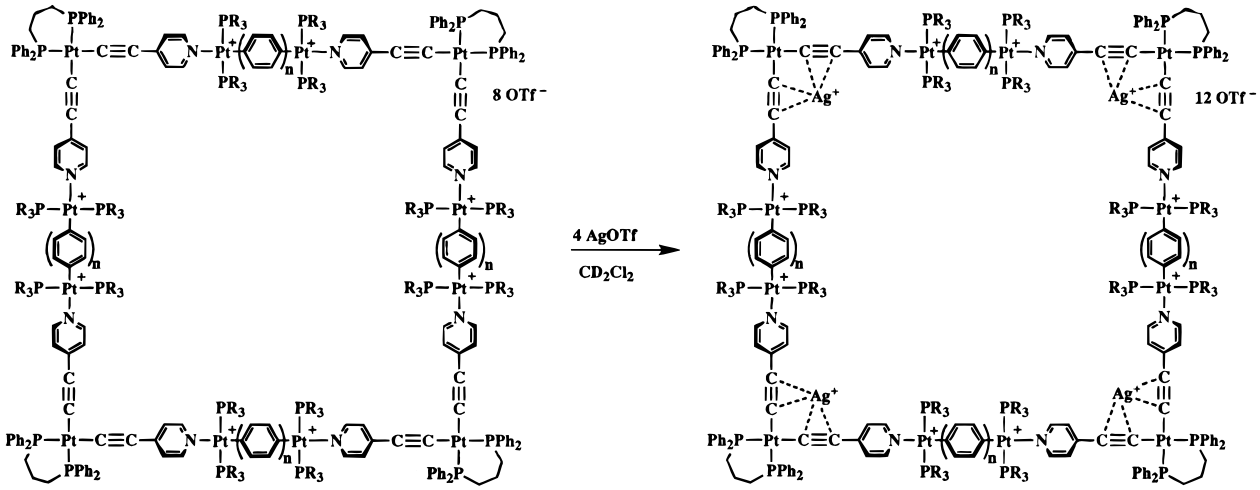

11: R = Et; n = 1
13: R = Ph; n = 2

17: R = Et; n = 1
18: R = Ph; n = 2

Competition Experiment. Insight into the nature of the self-assembly process and stability of these macrocycles can be obtained by performing a simple experiment. We were interested in determining whether there is any preferential selectivity for formation of one macrcocycle over another. Specifically, we monitored the reaction between a solid mixture of 0.5 equiv of each of both linear linkers **6** and **7** with 1.0 equiv of the corner **10**, dissolved in CD_2Cl_2 with dropwise addition. Statistically, there are six possible macrocycles that could form. Two of the products should be the pure squares **12** and **13**. While the other four possible systems would have a mixture of linkers **6** and **7** with corner **10**. Indeed, the observed product distribution, as best we can determine, is a mixture of the six possible squares, as indicated by the complex $^{31}P\{^1H\}$ and ^1H NMR data. We would have only expected to observe pure macrocycles **12** and **13** if the phosphine ligands (PEt_3 versus PPh_3) would manifest some enhanced electronic and/or steric stability to the pure macrocycles over the linker mixed macrocycles. It is interesting that we observe no oligomer formation. This suggests that the nature of the phosphine is not a critical parameter for macrocycle formation.

Conclusion

Two types of nanoscale metallocyclic molecular squares are reported. The first kind employs alkynylpyridine-containing angular building blocks as shape defining and -directing units. The second type uses bis*(*heteroaryliodonium) salts as corner units. These novel supramolecular species are formed in quantitative yields as assessed by NMR via spontaneous self-assembly of these angular corner units with diverse bimetallic linear linkers via dative bonding and the coordination motif. ESI−FTICR mass spectral data unambiguously establish the tetrameric nature of these molecules and, in conjunction with multinuclear NMR and physical data, their exact structure. Force field calculations and modeling establish the size of these species as ranging from approximately 3.6 to 4.7 nm (diagonally) and 2.6 to 3.4 nm (side) and, hence, the structures as true nanoscale supramolecular species.

Experimental Section

General Methods. All experiments were performed under an inert atmosphere of nitrogen utilizing standard Schlenk and glovebox techniques. Solvents used in the reactions were reagent or HPLC grade and purified in the following manner: toluene was distilled from sodium metal, methylene chloride was distilled from calcium hydride, and acetone was distilled from potassium permanganate. All NMR solvents (CD_2Cl_2, $CDCl_3$, and acetone-d_6) were stored over 4 Å molecular sieves in a drybox prior to use.

Platinum tetrakis(triphenylphosphine), silver trifluoromethanesulfonate (AgOTf), and bis[4-(4′-pyridyl)phenyl]iodonium trifluoromethanesulfonate were prepared by the standard literature procedures. 4,4′-Diiodobiphenyl was purchased from Aldrich and purified by recrystallization from chloroform.

All NMR spectra were obtained at room temperature with a Varian XL-300 or VXR-500 spectrometer employing a deuterium sample as an internal lock unless noted otherwise. The operating frequencies of the former spectrometer for the ^1H, $^{13}C\{^1H\}$, $^{31}P\{^1H\}$, and $^{19}F\{^1H\}$ NMR spectra were 300.0, 75.4, 121.4, and 282.3 MHz, respectively. For the latter spectrometer, the operating frequencies of the ^1H and $^{13}C\{^1H\}$ NMR spectra were 499.8 and 125.7 MHz, respectively. The ^1H chemical shifts are reported relative to the residual nondeuterated solvent of CD_2Cl_2 (5.32 ppm), $CDCl_3$ (7.27 ppm), or acetone-d_6 (2.05 ppm). The $^{13}C\{^1H\}$ chemical shifts are reported relative to $CDCl_3$ (77.0 ppm), CD_2Cl_2 (53.8 ppm), or acetone-d_6 (29.9 ppm). In contrast to the ^1H and $^{13}C\{^1H\}$ NMR spectra, the $^{31}P\{^1H\}$ and $^{19}F\{^1H\}$ NMR spectra were referenced to sealed external standards of 85% phosphoric acid and fluorotrichloromethane, respectively.

Elemental analyses were performed by Oneida Research Service, Whitesboro, NY, or Atlantic Microlab Inc., Norcross, GA. IR spectra were obtained with a Mattson Polaris FT-IR spectrometer at 2 cm^{-1} resolution. Melting points were obtained with a Mel-Temp capillary apparatus and are uncorrected.

Mass spectra of **5**−**8** were obtained with a Finnigan MAT 95 mass spectrometer employing a Finnigan MAT ICIS II operating system under positive ion fast atom bombardment (FAB) conditions at 8 keV. 3-Nitrobenzyl alcohol was used as a matrix in CH_2Cl_2 or $CHCl_3$ as solvent, and polypropylene glycol and cesium iodide were used as a reference for peak matching.

1,4-Bis(*trans*-Pt(PEt$_3$)$_2$(OSO$_2$CF$_3$))benzene (5). To a stirred solution of 4,4′-bis(*trans*-Pt(PEt$_3$)$_2$I)benzene (0.211 g, 0.177 mmol) in CH_2Cl_2 (10 mL) at 0 °C was added, AgOTf (0.049 g, 0.19 mmol) in the dark and under a nitrogen atmosphere; a light-yellow suspension immediately formed. After ∼2 h of stirring, the room-temperature suspension was cannula filtered to remove the AgI, and to the filtrate was added an equal volume of dry diethyl ether. The resulting solution was subsequently placed in the freezer for 1−2 days. The white, crystalline solid that formed was then filtered under nitrogen and dried *in vacuo* with slight heating (40 °C): yield 0.195 g (89%); mp 247−250 °C (dec.); IR (thin film, CD_2Cl_2, cm^{-1}) 2910, 2878 (C−H), 1436, 1418, 1383, 1094 (OTf); ^1H NMR (CD_2Cl_2) δ 6.79 (s, 4H, $^3J_{HPt}$ = 70 Hz), 1.63 (m, 24H, PCH_2CH$_3$), 1.12 (m, 36H, PCH$_2$CH_3); $^{13}C\{^1H\}$ NMR δ 136.1 (s, C$_o$−Pt), 120.2 (q, $^1J_{CF}$ = 319 Hz, OTf), 116.1 (s,

C_i−Pt), 14.0 (m, P*C*H$_2$CH$_3$), 8.0 (m, PCH$_2$*C*H$_3$); ^{31}P{^{1}H} NMR (CD$_2$Cl$_2$) δ 21.6 (s, $^1J_{PPt}$ = 2884 Hz); ^{19}F{^{1}H} NMR (CD$_2$Cl$_2$) δ −77.7 (s). Anal. Calcd for $C_{32}H_{64}F_6O_6P_4Pt_2S_2$: C, 31.07; H, 5.21; S, 5.18. Found: C, 31.16; H, 5.18; S, 5.10.

4,4′-Bis(*trans*-Pt(PEt$_3$)$_2$(OSO$_2$CF$_3$))biphenyl (6). To a stirred solution of 4,4′-bis(*trans*-Pt(PEt$_3$)$_2$I)biphenyl (0.166 g, 0.09 mmol) in CH$_2$Cl$_2$ (10 mL) at 0 °C was added AgOTf (0.049 g, 0.19 mmol) in the dark and under a nitrogen atmosphere; a light-yellow suspension immediately formed. After ∼2 h of stirring, the room-temperature suspension was cannula filtered to remove the AgI, and to the filtrate was added an equal volume of dry diethyl ether. The resulting solution was subsequently placed in the freezer for 1−2 days. The white, crystalline solid that formed was then filtered under nitrogen and dried *in vacuo* with slight heating (40 °C): yield 0.137 g (80%); mp 247−250 °C (dec.); IR (thin film, CD$_2$Cl$_2$, cm^{-1}) 2960, 2964 (C−H), 1309, 1232, 1170, 1037 (OTf); ^{1}H NMR (CD$_2$Cl$_2$) δ 7.29 (d, 4H, $^3J_{HH}$ = 8.4 Hz, $^3J_{HPt}$ = 76 Hz, H$_o$−Pt), 7.18 (d, 4H, $^3J_{HH}$ = 8.4 Hz, H$_m$−Pt), 1.65 (m, 24H, PC*H*$_2$CH$_3$), 1.13 (m, 36H, PCH$_2$C*H*$_3$); ^{13}C{^{1}H} NMR δ 136.6 (br s, C$_o$−Pt), 135.4 (s, C$_p$−Pt), 125.8 (s, $^3J_{CPt}$ = 80 Hz, C$_m$−Pt), 122.7 (t, $^2J_{CP}$ = 10 Hz, C$_i$−*P*t), 120.2 (q, $^1J_{CF}$ = 319 Hz, OTf), 14.1 (m, P*C*H$_2$CH$_3$), 8.0 (m, PCH$_2$*C*H$_3$); ^{31}P{^{1}H} NMR (CD$_2$Cl$_2$) δ 25.0 (s, $^1J_{PPt}$ = 2841 Hz); ^{19}F{^{1}H} NMR (CD$_2$Cl$_2$) δ −75.8 (s). Anal. Calcd for $C_{38}H_{68}F_6O_6P_4Pt_2S_2$: C, 34.76; H, 5.22; S, 4.88. Found: C, 34.58; H, 5.18; S, 4.82.

4,4′-Bis(*trans*-Pt(PPh$_3$)$_2$(OSO$_2$CF$_3$))biphenyl (7). To a stirred solution of 4,4′-bis(*trans*-Pt(PPh$_3$)$_2$I)biphenyl (0.166 g, 0.09 mmol) in CH$_2$Cl$_2$ (13 mL) at −5 °C was added AgOTf (0.049 g, 0.19 mmol) in the dark and under a nitrogen atmosphere; a light-yellow suspension immediately formed. After ∼6 h of stirring, the room-temperature suspension was cannula filtered to remove the AgI, and the filtrate was obtained as a solid by evaporation of the colorless solution employing a flow of nitrogen. The white solid was then dried *in vacuo* with slight heating (40 °C). The crystalline product was obtained by slow evaporation of a concentrated chloroform solution at room temperature: yield 0.137 g (80%); mp 228−232 °C (dec.); IR (thin film, CD$_2$Cl$_2$, cm^{-1}) 3061 (C−H), 1434, 1470 (Ar), 1282, 1263, 1181, 1077 (OTf); ^{1}H NMR (CD$_2$Cl$_2$) δ 7.51 (m, 24H, H$_o$−P), 7.40 (t, 12H, $^3J_{HH}$ = 7.2 Hz, H$_p$−P), 7.30 (m, 24H, H$_m$−P), 6.40 (d, 4H, $^3J_{HH}$ = 8.2 Hz, $^3J_{HPt}$ = 60 Hz, H$_o$−Pt), 5.96 (d, 4H, $^3J_{HH}$ = 8.2 Hz, H$_m$−Pt); ^{13}C{^{1}H} NMR δ 135.6 (br s, C$_o$−Pt), 134.9 (t, $^2J_{CP}$ = 6.3 Hz, C$_o$−P), 130.6 (s, C$_p$−P), 128.9 (t, $^1J_{CP}$ = 28.1 Hz, C$_i$−P), 128.8 (s, C$_p$−Pt), 128.2 (t, $^3J_{CP}$ = 5.9 Hz, C$_m$−P), 125.9 (s, C$_m$−Pt), 122.4 (t, $^2J_{CP}$ = 8.1 Hz, C$_i$−Pt), 118.9 (q, $^1J_{CF}$ = 319 Hz, OTf); ^{31}P{^{1}H} NMR (CDCl$_3$) δ 29.3 (s, $^1J_{PPt}$ = 3219 Hz); ^{19}F{^{1}H} NMR (CDCl$_3$) δ −77.9 (s); FAB-MS *m*/*z* (rel intensity) 1740 (M − OTf$^+$, 100), 1478 (M − OTf − PPh$_3^+$, 68).

4,4″-Bis(*trans*-Pt(PPh$_3$)$_2$(OSO$_2$CF$_3$))-*p*-terphenyl (8). To a stirred suspension of 4,4′-bis(*trans*-Pt(PPh$_3$)$_2$I)-*p*-terphenyl (0.251 g, 0.13 mmol) in cooled CH$_2$Cl$_2$ (5 °C, 18 mL) was added AgOTf (0.71 g, 0.27 mmol) in the dark and under a nitrogen atmosphere. Immediately after addition of AgOTf, the ice bath was removed, and the reaction was allowed to warm to room temperature. After ∼2.5 h of stirring, light-yellow suspension was cannula filtered to remove the AgI, and the filtrate was obtained as a solid by evaporation of the colorless solution employing a flow of nitrogen. The solid was dried *in vacuo* at ∼40 °C for 4 h (Yield 0.202 g, 79%). The white solid was found to be only partially soluble in chloroform or methylene chloride. Microcrystalline product could be obtained, with considerable difficulty, by first dissolving the solid into methylene chloride (∼20 mL) followed by addition of dry toluene (∼8 mL). Nitrogen gas was subsequently passed over the solution at room temperature; after slow evaporation of the liquid phase to half volume, pure microcrystals were obtained: yield 0.129 g (50%); mp 230−232 °C (dec.); IR (mull, fluorolube, cm^{-1}) 3051 (C−H); ^{1}H NMR (CD$_2$Cl$_2$) δ 7.50 (m, 24H, H$_o$−P), 7.43 (t, 12H, $^3J_{HH}$ = 7.3 Hz, H$_p$−P), 7.33 (m, 24H, H$_m$−P), 7.20 (s, 4H, H$_\gamma$), 6.55 (d, 4H, $^3J_{HH}$ = 8.4 Hz, H$_o$−Pt), 6.29 (d, 4H, $^3J_{HH}$ = 8.4 Hz, H$_m$−Pt); ^{31}P{^{1}H} NMR (CDCl$_3$) δ 29.3 (s, $^1J_{PPt}$ = 3198 Hz); ^{19}F{^{1}H} NMR (CDCl$_3$) δ −78.0 (s); FAB-MS *m*/*z* (ion, rel intensity) 1817.6 (M − OTf$^+$, 100), 1555.3 (M − OTf − PPh$_3^+$, 30).

Cyclotetrakis[[*cis*-Pt(dppp)(4-ethynylpyridine)$_2$][1,4-bis(*trans*-Pt(PEt$_3$)$_2$(OTf))benzene]] (11). A room temperature methylene chloride solution (0.7 mL) of bis(4-ethynylpyridyl)platinum)-1,3-bis-(diphenylphosphino)propane (0.0131 g, 0.0162 mmol) was added dropwise to solid 4,4′-bis(*trans*-Pt(PEt$_3$)$_2$(OSO$_2$CF$_3$))biphenyl (0.0200 g, 0.0162 mmol) with stirring in the drybox. The self-assembly was monitored by ^{1}H and ^{31}P{^{1}H} NMR spectroscopy and determined to be complete, and the yield of the macrocycle was quantitative, after 1 h. The light-orange solution was then dried *in vacuo* yielding an orange-colored solid: yield 0.0311 g (94%); mp 302−304 °C (dec.); IR (thin film, CD$_2$Cl$_2$, cm^{-1}) 3340, 3123 (C−H), 2116 (C≡C), 1603, 1487, 1437 (Ar), 1271, 1158, 1104, 1032 (OTf); ^{1}H NMR (300 MHz, CD$_2$Cl$_2$) δ 8.20 (d, $^3J_{HH}$ = 5.7 Hz, 16H, H$_\alpha$−Py), 7.68, 7.43 (m, 80H, HP), 6.96 (s, 16H, H$_o$−Pt), 6.88 (d, 16H, $^3J_{HH}$ = 6.3 Hz, H$_\beta$−Py), 2.65 (br s, 16H, CH$_2$C*H*$_2$P-dppp), 2.08 (br s, 8H, C*H*$_2$CH$_2$P-dppp), 1.26 (m, 96H, PC*H*$_2$CH$_3$), 1.08 (m, 144H, PCH$_2$C*H*$_3$); ^{13}C{^{1}H} NMR (125.7 MHz, CD$_2$Cl$_2$) δ 150.8 (s, C$_\alpha$−Py), 138.9 (s, C$_\gamma$−Py), 137.1 (s, C$_o$−Pt), 133.9 (br s, C$_o$−PPh$_2$), 131.5 (s, C$_p$−PPh$_2$), 130.7 (m, C$_i$−PPh$_2$), 129.2 (s, C$_\beta$−Py), 129.1 (s, C$_m$−PPh$_2$), 125.5 (br s, C≡C$_\alpha$−Pt), 121.6 (q, $^1J_{CF}$ = 314 Hz, OTf), (Pt−C$_i$ not observed), 107.4 (m, C≡C$_\beta$−Pt), 25.5 (m, CH$_2$C*H*$_2$P-dppp), 20.0 (br s, C*H*$_2$CH$_2$P-dppp), 12.9 (t, J_{CP}= 20 Hz, P*C*H$_2$CH$_3$), 7.9 (s, PCH$_2$*C*H$_3$); ^{31}P{^{1}H} NMR (CD$_2$Cl$_2$) δ 14.3 (s, 16P, $^1J_{PPt}$ = 2722 Hz, PEt$_3$), −5.8 (s, 8P, $^1J_{PPt}$ = 2171 Hz, PPh$_2$); ^{19}F{^{1}H} NMR (CD$_2$Cl$_2$) δ −77.9 (s). Anal. Calcd for $C_{292}H_{392}F_{24}N_8O_{24}P_{24}Pt_{12}S_8$: C, 42.81; H, 4.82; N, 1.37; S, 3.13. Found: C, 42.68; H, 4.91; N, 1.34; S, 3.10.

Cyclotetrakis[[*cis*-Pt(dppp)(4-ethynylpyridine)$_2$][4,4′-bis(*trans*-Pt(PEt$_3$)$_2$(OTf))biphenyl]] (12). A room temperature methylene chloride solution (0.7 mL) of (bis(4-ethynylpyridyl)platinum)-1,3-bis-(diphenylphosphino)propane (0.0131 g, 0.0162 mmol) was added dropwise to solid 4,4′-bis(*trans*-Pt(PEt$_3$)$_2$(OSO$_2$CF$_3$))biphenyl (0.0212 g, 0.0162 mmol) with stirring in the drybox. The self-assembly was monitored by ^{1}H and ^{31}P{^{1}H} NMR spectroscopy and determined to be complete, and the yield of the macrocycle was quantitative, after 1 h. The light-orange solution was then dried *in vacuo* yielding a light-yellow solid: yield 0.0333 g (97%); mp 255−260 °C (dec.); IR (thin film, CD$_2$Cl$_2$, cm^{-1}) 3055, 2967 (C−H), 2118 (C≡C), 1603, 1486, 1436 (Ar), 1268, 1151, 1102, 1031 (OTf); ^{1}H NMR (300 MHz, CD$_2$Cl$_2$) δ 8.23 (d, $^3J_{HH}$ = 6.4 Hz, 16H, H$_\alpha$−Py), 7.69, 7.43, 7.34 (m, 112H, HP, H$_o$−Pt, H$_m$−Pt), 6.90 (d, 16H, $^3J_{HH}$ = 6.4 Hz, H$_\beta$−Py), 2.66 (br s, 16H, C*H*$_2$CH$_2$P-dppp), 2.11 (br s, 8H, C*H*$_2$CH$_2$P-dppp), 1.28 (m, 96H, PC*H*$_2$-CH$_3$), 1.07 (m, 144H, PCH$_2$C*H*$_3$); ^{13}C{^{1}H} NMR (125.7 MHz; CD$_2$-Cl$_2$) δ 150.8 (s, C$_\alpha$−Py), 139.04 (s, C$_\gamma$−Py), 136.7 (s, C$_o$−Pt), 136.1 (s, C$_p$−*P*t), 133.9 (br s, C$_o$−PPh$_2$), 131.5 (s, C$_p$−PPh$_2$), 131.0 (m, C$_i$−PPh$_2$), 129.3 (s, C$_\beta$−Py), 129.10 (s, C$_m$−PPh$_2$), 126.3 (s, C$_m$−Pt), 121.6 (q, $^1J_{CF}$ = 322 Hz, OTf), (C≡C$_\alpha$−Pt and Pt−C$_i$ not observed), 107.4 (m, C≡C$_\beta$−Pt), 25.5 (m, CH$_2$C*H*$_2$P-dppp), 20.0 (br s, C*H*$_2$CH$_2$P-dppp), 12.8 (t, J_{CP} = 20 Hz, P*C*H$_2$CH$_3$), 7.9 (s, PCH$_2$*C*H$_3$); ^{31}P{^{1}H} NMR (CD$_2$Cl$_2$) δ 16.45 (s, 16P, $^1J_{PPt}$ = 2699 Hz, PEt$_3$), −4.47 (s, 8P, $^1J_{PPt}$ = 2185 Hz, PPh$_2$); ^{19}F{^{1}H} NMR (CD$_2$Cl$_2$) δ −76.5 (s). Anal. Calcd for $C_{316}H_{408}F_{24}N_8O_{24}P_{24}Pt_{12}S_8$: C, 44.66; H, 4.84; N, 1.32; S, 3.02. Found: C, 43.61; H, 4.79; N, 1.33; S, 3.01.

Cyclotetrakis[[*cis*-Pt(dppp)(4-ethynylpyridine)$_2$][4,4′-bis(*trans*-Pt(PPh$_3$)$_2$(OTf))biphenyl]] (13). A room temperature methylene chloride solution (0.7 mL) of (bis(4-ethynylpyridyl)platinum)-1,3-bis-(diphenylphosphino)propane (0.0180 g, 0.0220 mmol) was added dropwise to solid 4,4′-bis(*trans*-Pt(PPh$_3$)$_2$(OSO$_2$CF$_3$))biphenyl (0.0411 g, 0.0218 mmol) with stirring in the drybox. The self-assembly was monitored by ^{1}H and ^{31}P{^{1}H} NMR spectroscopy and determined to be complete, and the yield of the macrocycle was quantitative, after 1 h. The light-orange solution was then dried *in vacuo* yielding a light-yellow solid: yield 0.035 g (58%); mp 215−220 °C (dec.); IR (thin film, CD$_2$Cl$_2$, cm^{-1}) 3076, 3054 (C−H), 2119 (C≡C), 1605, 1587, 1482, 1435 (Ar), 1265, 1150, 1100, 1030 (OTf); ^{1}H NMR (300 MHz, CD$_2$Cl$_2$) δ 7.65 (m, 32H, HP), 7.53 (d, $^3J_{HH}$ = 6.5 Hz, 16H, H$_\alpha$−Py), 7.39, 7.28, 7.18 (m, 288H, HP), 6.67 (d, 16H, $^3J_{HH}$ = 8.1 Hz, H$_o$−Pt), 6.30 (d, 16H, $^3J_{HH}$ = 8.1 Hz, H$_m$−Pt), 5.87 (d, 16H, $^3J_{HH}$ = 6.4 Hz, H$_\beta$−Py), 2.53 (br s, 16H, PC*H*$_2$CH$_3$), 2.04 (br s, 8H, PCH$_2$C*H*$_3$); ^{13}C{^{1}H} NMR (125.7 MHz, CD$_2$Cl$_2$) δ 150.5 (s, C$_\alpha$−Py), 137.9 (s, C$_o$−Pt), 137.4 (br s, C$_\gamma$−Py), 136.5 (s, C$_p$−Pt), 134.5 (t, $^2J_{CP}$ = 5.8 Hz, C$_o$−PPh$_3$), 133.9 (br s, C$_o$−PPh$_2$), 131.7 (s, C$_p$−PPh$_2$), 131.4 (s, C$_p$−PPh$_3$), 131.0 (m, C$_i$−PPh$_2$), 129.1 (t, $^3J_{CP}$ = 5.2 Hz, C$_m$−PPh$_3$ and PPh$_2$), 128.0 (t, $^1J_{CP}$ = 25.4 Hz, C$_i$−PPh$_3$), 127.8 (s, C$_\beta$−Py), ∼128 (obscured, C$_i$−Pt), 126.4 (s, C$_m$−Pt), 121.8 (q, $^1J_{CF}$ = 321 Hz, OTf), 122.0 (m, C≡C$_\alpha$−Pt), 107.1 (m, C≡C$_\beta$−Pt), 26.1 (m, CH$_2$C*H*$_2$P-dppp),

20.3 (br s, *C*H$_2$CH$_2$P-dppp); ^{31}P{^{1}H} NMR (CD$_2$Cl$_2$) δ 21.4 (s, 16P, $^1J_{PPt}$ = 3060 Hz, PPh$_3$), −5.5 (s, 8P, $^1J_{PPt}$ = 2198 Hz, PPh$_2$); ^{19}F{^{1}H} NMR (CDCl$_3$) δ −78 (s). Anal. Calcd for $C_{508}H_{408}F_{24}N_8O_{24}P_{24}Pt_{12}S_8$: C, 56.47; H, 3.81; N, 1.04. Found: C, 55.32; H, 3.89; N, 1.04.

Cyclotetrakis[[*cis*-Pt(dppp)(4-ethynylpyridine)$_2$][4,4″-bis(*trans*-Pt(PPh$_3$)$_2$(OTf))-*p*-terphenyl]] (14). A 0.6 mL methylene chloride-d_2 solution of light-yellow (bis(4-ethynylpyridyl)platinum)-1,3-bis-(diphenylphosphino)propane (0.0062 g, 0.0076 mmol) was added dropwise to solid, colorless 4,4″-bis(*trans*-Pt(PPh$_3$)$_2$(OSO$_2$CF$_3$))-*p*-terphenyl (0.0150 g, 0.0076 mmol) with stirring in the drybox. The self-assembly was monitored by ^{1}H and ^{31}P{^{1}H} NMR spectroscopy and determined to be complete, and the yield of the macrocycle was quantitative, after 1.25 h. The light-orange product solution was then dried *in vacuo* yielding a yellow solid: yield 0.0182 g (86%); mp 230−234 °C (dec.); IR (thin film, CD$_2$Cl$_2$, cm^{-1}) 3057 (C−H), 2117 (C≡C), 1605, 1483, 1434 (Ar), 1266, 1150, 1100, 1030 (OTf); ^{1}H NMR (300 MHz, CD$_2$Cl$_2$) δ 7.65 (m, 32H, HP), 7.57 (d, $^3J_{HH}$ = 6.2 Hz, 16H, H$_\alpha$−Py), 7.40, 7.32, 7.25 (m, 288H, HP), ∼7.23 (obscured H$_\gamma$), 6.78 (d, 16H, $^3J_{HH}$ = 8.2 Hz, H$_o$−Pt), 6.57 (d, 16H, $^3J_{HH}$ = 8.2 Hz, H$_m$−Pt), 5.90 (d, 16H, $^3J_{HH}$ = 6.2 Hz, H$_\beta$−Py), 2.52 (br s, 16H, CH$_2$C*H*$_2$P-dppp), 2.05 (br s, 8H, C*H*$_2$CH$_2$P-dppp); ^{13}C{^{1}H} NMR (125.7 MHz, CD$_2$Cl$_2$) δ 150.5 (s, C$_\alpha$−Py), 140.1 (s, *p*-C$_6$H$_4$−C$_i$), 138.2 (s, C$_o$−Pt), 137.4 (br s, C$_\gamma$−Py), 135.5 (s, C$_p$−*P*t), 134.5 (t, $^2J_{CP}$ = 5.5 Hz, C$_o$−PPh$_3$), 134.0 (br s, C$_o$−PPh$_2$), 131.7 (s, C$_p$−PPh$_2$), 131.5 (s, C$_p$−PPh$_3$), 130.8 (m, C$_i$−PPh$_2$), 129.3 (t, $^3J_{CP}$ = 5.2 Hz, C$_m$−PPh$_3$ and PPh$_2$), 127.9 (t, $^1J_{CP}$ = 28.2 Hz, C$_i$−PPh$_3$), 127.9 (s, C$_\beta$−Py), ∼128 (obscured, C$_i$−Pt), 127.0 (s, *p*-C$_6$H$_4$−C$_o$), 126.5 (s, C$_m$−Pt), 121.8 (q, $^1J_{CF}$ = 321 Hz, OTf), 122.0 (m, C≡C$_\alpha$−Pt), 107.1 (m, C≡C$_\beta$−Pt), 26.2 (m, CH$_2$*C*H$_2$P-dppp), 20.4 (br s, *C*H$_2$CH$_2$P-dppp); ^{31}P{^{1}H} NMR (CD$_2$Cl$_2$) δ 21.3 (s, 16P, $^1J_{PPt}$ = 3049 Hz, PPh$_3$), −5.7 (s, 8P, $^1J_{PPt}$ = 2197 Hz, PPh$_2$); ^{19}F{^{1}H} NMR (CD$_2$Cl$_2$) δ −78 (s). Anal. Calcd for $C_{532}H_{424}F_{24}N_8O_{24}P_{24}Pt_{12}S_8$: C, 57.51; H, 3.85; N, 1.01. Found: C, 57.12; H, 3.93; N, 1.00.

Cyclotetrakis[[bis(4-(4′-pyridyl)phenyl)iodonium(OTf)][1,4-bis-(*trans*-Pt(PEt$_3$)$_2$(OTf))benzene]] (15). To a room temperature acetone/methylene chloride (4:3 mL) solution of 4,4′-bis(*trans*-Pt(PEt$_3$)$_2$(OSO$_2$-CF$_3$))benzene (0.020 g, 0.0162 mmol) was added dropwise, with stirring, a suspension of bis[4-(4′-pyridyl)phenyl]iodonium triflate (0.094 g, 0.0162 mmol) in acetone/methylene chloride (3:2 mL). After for 6 h of stirring in the drybox, the light-orange solution was filtered and then dried *in vacuo* yielding a light-orange solid. When monitored by ^{1}H and ^{31}P{^{1}H} NMR spectroscopy, the reaction is determined to be quantitative. For **15**: yield: 0.050 g (81%); mp 202−205 °C (dec.); IR (thin film, acetone-d_6, cm^{-1}) 3058 (C−H), 1393, 1435, 1480 (Ar), 1276, 1260, 1155, 1098 (OTf); ^{1}H NMR (499.8 MHz, acetone-d_6) δ 8.98 (d, 16H, $^3J_{HH}$ = 5.7 Hz, H$_\alpha$−Py), 8.54 (d, 16H, $^3J_{HH}$ = 8.4 Hz, H$_\alpha$−PhI), 8.10 (m, 32H, H$_\beta$−PhI and H$_\beta$−Py), 7.13 (s, H$_o$−Pt), 1.42 (m, 96H, PC*H*$_2$CH$_3$), 1.12 (m, 144H, PCH$_2$C*H*$_3$); ^{13}C{^{1}H} NMR (125.7 MHz, acetone-d_6) δ 153.5 (s, C$_\alpha$−Py), 149.0 (s, C$_\gamma$−Py), 140.5 (s, C$_\gamma$−PhI), 137.4 (s, C$_\alpha$−PhI), 137.1 (s, C$_o$−Pt), 131.6 (s, C$_\beta$−PhI), 128.1 (t, $^2J_{CP}$ = 9 Hz, C$_i$−Pt), 126.0 (s, C$_\beta$−Py), 121.7 (q, $^1J_{CF}$ = 322 Hz, OTf), 116.4 (s, C$_i$−PhI); ^{31}P{^{1}H} NMR (acetone-d_6) δ 14.2 (s, $^1J_{PPt}$ = 2720 Hz); ^{19}F{^{1}H} NMR (CDCl$_3$) δ −77 (s).

Cyclotetrakis[[bis(4-(4′-pyridyl)phenyl)iodonium(OTf)][4,4′-bis-(*trans*-Pt(PPh$_3$)$_2$(OTf))biphenyl]] (16). To a room temperature acetone/methylene chloride (4:3 mL) solution of 4,4′-bis(*trans*-Pt(PPh$_3$)$_2$(OSO$_2$-CF$_3$))biphenyl (0.0500 g, 0.025 mmol) was added dropwise, with stirring, a suspension of bis[4-(4′-pyridyl)phenyl]iodonium triflate (0.0145 g, 0.025 mmol) in acetone/methylene chloride (3:2 mL). After 6 h of stirring in the drybox, the light-orange solution was filtered and then dried *in vacuo* yielding a light-orange solid. When monitored by ^{1}H and ^{31}P{^{1}H} NMR spectroscopy, the reaction is determined to be quantitative. For **16**: yield 0.050 g (81%); mp 202−205 °C (dec.); IR (thin film, acetone-d_6, cm^{-1}) 3058 (C−H), 1393, 1435, 1480 (Ar), 1276, 1260, 1155, 1098 (OTf); ^{1}H NMR (499.8 MHz, acetone-d_6) δ 8.52 (d, 16H, partially obscured, H$_\alpha$−Py), 8.49 (d, 16H, $^3J_{HH}$ = 8.5 Hz, H$_\alpha$−PhI), 7.69 (d, 16H, $^3J_{HH}$ = 8.5 Hz, H$_\beta$−PhI), 7.50 (m, 96H, H$_o$−P), 7.40 (t, 48H, $^3J_{HH}$ = 7.2 Hz, H$_p$−P), 7.32 (m, 96H, H$_m$−P), 7.18 (d, 16H, $^3J_{HH}$ = 6.5 Hz, H$_\beta$−Py), 6.82 (d, 16H, $^3J_{HH}$ = 8.0 Hz, H$_o$−Pt), 6.35 (d, 16H, $^3J_{HH}$ = 8.0 Hz, H$_m$−Pt); ^{13}C{^{1}H} NMR (125.7 MHz, acetone-d_6) δ 153.6 (s, C$_\alpha$−Py), 148.3 (s, C$_\gamma$−Py), 141.3 (s, C$_\gamma$−PhI), 138.6 (s, C$_\alpha$−PhI), 137.7 (s, C$_o$−Pt), 136.8 (s, C$_p$−Pt), 135.2 (t, $^2J_{CP}$ = 6.0 Hz, C$_o$−P), 131.8 (s, C$_p$−P), 131.6 (s, C$_\beta$−PhI), 129.6 (t, $^3J_{CP}$ = 5.2 Hz, C$_m$−P), 128.6 (t, $^1J_{CP}$ = 28.2 Hz, C$_i$−P), (C$_i$−Pt not observed), 126.3 (s, C$_m$−Pt), 124.9 (s, C$_\beta$−Py), 122.4 (q, $^1J_{CF}$ = 314 Hz, OTf), 116.7 (s, C$_i$−PhI), 12.9 (s, PC*H*$_2$CH$_3$), 7.8 (s, PCH$_2$*C*H$_3$); ^{31}P{^{1}H} NMR (acetone-d_6) δ 22.5 (s, $^1J_{PPt}$ = 3076 Hz); ^{19}F{^{1}H} NMR (CDCl$_3$) δ −75.2 (s); MALDI-MS *m*/*z* (rel intensity) 1500 (M − 6OTf$^+$); ESI-FTICR *m*/*z* (acetone) 1500.163 amu [M − 6OTf$^-$] (mass = 9000.98 obsd; mass = 9001.02 calcd).

Cyclotetrakis[[*cis*-Pt(dppp)(4-ethynylpyridine)$_2$][1,4-bis(*trans*-Pt(PEt$_3$)$_2$(OTf))benzene]]·4AgOTf (17). A methylene chloride-d_2 solution (0.8 mL) of macrocycle **11** (0.0331 g, 0.0041 mmol) at room temperature was added dropwise to a vial containing solid AgOTf (0.0042 g, 0.0162 mmol) in the drybox. The resulting orange-yellow solution was filtered through a short plug of glass wool after for 15 min of stirring. The reaction was found to be quantitative and yield the single desired silver adduct, as determined by NMR spectroscopy. For **17**: yield 0.0347 g (93%); mp 214−220 °C (dec.); IR (thin film, CD$_2$Cl$_2$, cm^{-1}) 3055, 2925 (C−H), 2086 (C≡C), 1606, 1587, 1481, 1436 (Ar), 1266, 1205, 1100, 1030 (OTf); ^{1}H NMR (500 MHz, CD$_2$Cl$_2$) δ 8.23 (d, $^3J_{HH}$ = 3.9 Hz, 16H, H$_\alpha$−Py), 7.69 (m, 32H, PPh$_2$), 7.44 (m, 48H, PPh$_2$), 6.97 (s, 16H, H$_o$−Pt), 6.94 (d, 16H, $^3J_{HH}$ = 3.3 Hz, H$_\beta$−Py), 2.73 (br s, 16H, CH$_2$C*H*$_2$P-dppp), 2.13 (br s, 8H, C*H*$_2$-CH$_2$P-dppp), 1.25 (m, 96H, PC*H*$_2$CH$_3$), 1.04 (m, 144H, PCH$_2$C*H*$_3$); ^{13}C{^{1}H} NMR (125.7 MHz, CD$_2$Cl$_2$) δ 150.9 (s, C$_\alpha$−Py), 137.0 (s, C$_o$−Pt), 135.5 (s, C$_\gamma$−Py), 134.0 (br s, C$_o$−PPh$_2$), 131.9 (s, C$_p$−PPh$_2$), 130.1 (s, C$_\beta$−Py), 129.4 (s, C$_m$−PPh$_2$), 129.0 (m, C$_i$−PPh$_2$), 125.4 (br s, C≡C$_\alpha$−Pt), 121.3 (q, $^1J_{CF}$ = 322 Hz, OTf), (Pt−C$_i$ not observed), 109.0 (m, C≡C$_\beta$−Pt), 24.9 (m, CH$_2$*C*H$_2$P-dppp), 19.8 (br s, *C*H$_2$CH$_2$P-dppp), 12.9 (t, J_{CP}= 20 Hz, P*C*H$_2$CH$_3$), 7.9 (s, PCH$_2$*C*H$_3$); ^{31}P{^{1}H} NMR (CD$_2$Cl$_2$) δ 13.3 (s, 16P, $^1J_{PPt}$ = 2723 Hz, PEt$_3$), −9.2 (s, 8P, $^1J_{PPt}$ = 2338 Hz, PPh$_2$); ^{19}F{^{1}H} NMR (CDCl$_3$) δ −75.4 (s). Anal. Calcd for $C_{220}H_{320}F_{36}I_4N_8O_{36}P_{16}Pt_8S_{12}$: C, 38.55; H, 4.28; N, 1.21; S, 4.17. Found: C, 38.65; H, 4.31; N, 1.19; S, 4.10.

Cyclotetrakis[[*cis*-Pt(dppp)(4-ethynylpyridine)$_2$][4,4′-bis(*trans*-Pt(PPh$_3$)$_2$(OTf))biphenyl]]·4AgOTf (18). A methylene chloride-d_2 solution (0.8 mL) of macrocylce **13** (0.0472 g, 0.0037 mmol) at room temperature was added dropwise to a vial containing solid AgOTf (0.0046 g, 0.0180 mmol) in the glovebox. The slightly darkened, orange-yellow solution was filtered through a short plug of glass wool after for 15 min of stirring. The reaction was found to be quantitative and yield the single desired silver adduct, as determined by NMR spectroscopy. The solid was dried *in vacuo* and stored under vacuum in the dark: yield 0.0471 g (91%); mp 214−220 °C (dec.); IR (thin film, CD$_2$Cl$_2$, cm^{-1}) 3055, 2925 (C−H), 2086 (C≡C), 1606, 1587, 1481, 1436 (Ar), 1266, 1205, 1100, 1030 (OTf); ^{1}H NMR (300 MHz, CD$_2$Cl$_2$) δ 7.65 (m, 32H, HP), 7.52 (d, $^3J_{HH}$ = 5.8 Hz, 16H, H$_\alpha$−Py), 7.42, 7.29, 7.25 (m, 288H, HP), 6.70 (d, 16H, $^3J_{HH}$ = 7.9 Hz, H$_o$−Pt), 6.31 (d, 16H, $^3J_{HH}$ = 7.9 Hz, H$_m$−Pt), 5.83 (d, 16H, $^3J_{HH}$ = 6.4 Hz, H$_\beta$−Py), 2.60 (br s, 16H, CH$_2$C*H*$_2$P-dppp), 2.07 (br s, 8H, C*H*$_2$CH$_2$P-dppp); ^{13}C{^{1}H} NMR (125.7 MHz, CD$_2$Cl$_2$) δ 150.6 (s, C$_\alpha$−Py), 137.9 (s, C$_o$−Pt), 136.5 (s, C$_p$−*P*t), 134.4 (br s, C$_o$−PPh$_3$), 133.94 (br s, C$_o$−PPh$_2$), ∼133.6 (partially obscured, C$_\gamma$−Py), 132.2 (s, C$_p$−PPh$_2$), 131.5 (s, C$_p$−PPh$_3$), 129.6 (s, C$_m$−PPh$_2$), 129.2 (br s, C$_m$−PPh$_3$), ∼129−130 (C$_i$−PPh$_2$ obscured), 128.6 (s, C$_\beta$−Py), 127.9 (t, $^1J_{CP}$ = 28.2 Hz, C$_i$−PPh$_3$), ∼128−131 (obscured, C$_i$−Pt), 126.4 (s, C$_m$−Pt), 121.54 (q, $^1J_{CF}$ = 321 Hz, OTf), (not observed, C≡C$_\alpha$−Pt), 108.7 (m, C≡C$_\beta$−Pt), 25.4 (m, CH$_2$*C*H$_2$P-dppp), 19.9 (br s, *C*H$_2$CH$_2$P-dppp); ^{31}P{^{1}H} NMR (CD$_2$Cl$_2$) δ 20.5 (s, 16P, $^1J_{PPt}$ = 3048 Hz, PPh$_3$), −9.0 (s, 8P, $^1J_{PPt}$ = 2359 Hz, PPh$_2$); ^{19}F{^{1}H} NMR (CDCl$_3$) δ −76.3 (s). Anal. Calcd for $C_{512}H_{408}Ag_4F_{36}N_8O_{36}P_{24}Pt_{12}S_{12}$: C, 51.97; H, 3.48; N, 0.95. Found: C, 51.37; H, 3.65; N, 0.92.

Electrospray Ionization Fourier Transform (ESI-FTICR) Mass Spectrometry of Macrocycles 13 and 16. The electrospray ionization (ESI) Fourier transform ion cyclotron resonance (FTICR) mass spectrometer used for the present study is based on data collected with an Oxford 7 T superconducting magnet. A full description of this instrumental technique has been provided in detail elsewhere.[14−17]

Macrocycle **13** (ca. 1 mg/mL in CH$_2$Cl$_2$) was electrosprayed at a flow rate of 0.3 μL/min with a source potential of ca. 3 kV to produce a stable positive ion current. The resistively heated desolvation capillary temperature was reduced to 35 °C, and the capillary-skimmer potential was reduced to 30 V; both parameters were decreased to avoid thermal

or collisional dissociation, respectively, and correspond to very gentle source conditions. To enhance the signal-to-noise and dynamic range, selected ion accumulation (i.e., quadrupolar excitation at a single frequency) was employed for ion accumulation during the ion injection event. Specifically, to enhance the signal of the 5+ charge state of macrocycle **13**, a wave form was applied at $m/z = 2012$ at 0.7 V peak-to-peak. The selected ion accumulation of only the 5+ charge states results from the magnetron ejection of other species in the ICR cell during the relatively high pressure ($\sim 10^{-4}$ Torr) associated with the accumulation/pulsed valve event. The determined mass of the 5+ ion was 10 060.15 Da (theoretical mass of 10 060.03 Da; error = 12 ppm).

A sample of **16** was prepared by dissolving it in acetone just prior to analysis. The sample (ca. 1 mg/mL) was then loaded into a 10 mL Hamilton syringe, placed into a Harvard syringe pump, and introduced into the mass spectrometer at a flow rate of 0.3 mL/min.[3] The resistively heated desolvation capillary was reduced to 2 A, and the capillary-skimmer potential was reduced to 20 V; both parameters were decreased to avoid thermal or collisional dissociation and correspond to very gentle conditions. A source potential of ca. 2.5 kV was applied to produce a stable positive ion current. A quadruple excitation wave form was applied for selected ion accumulation at *m/z* 1500. The ESI−FTICR−MS spectrum of **16** was obtained with an injection/accumulation time of 10 s. The determined mass of the 6+ ion was 9000.98 Da (theoretical mass of **16**, 9001.02 Da; error = 4.4 ppm).

Tandem Mass Spectrometry of 13. The selected 5+ charge state of macrocycle **13** was subsequently collisionally activated inside the ICR using a sustained off-resonance irradiation (SORI) event in the presence of a buffer gas (e.g., N_2). The SORI event was applied −500 Hz off-resonance at 25 dB for a duration of 0.25 s. The total experiment time including the ion injection and pump down sequences lasted 17 s. The fragment ions of the intact macrocycle were then identified which was facilitated by the direct charge state determination approach based upon the ability of the FTICR to resolve the isotopic envelope.

General Procedure for Exchange Experiments. Each macrocycle that was studied was prepared in the drybox in the appropriate solvent according to the given procedure (*vide supra*). After reaction completion, the preformed square was added as a solution to a 4-fold excess of the solid competitor moiety. The progress of the exchange was monitored periodically by ^{1}H and ^{31}P NMR spectroscopies.

Acknowledgment. Dedicated to Professor Albert I. Meyers on the occasion of his 65th birthday. Financial support by the NSF (CHE-9529093), NIH (2ROCA16903), and the University of Utah Institutional Funds Committee as well as the generous loan of platinum(II) dichloride from Johnson-Matthey are gratefully acknowledged.

JA972668S